Conformational Structure of Some Trimeric and Pentameric Structural Units of Heparin

Milan Remko*,†,‡ and Claus-Wilhelm von der Lieth‡

Department of Pharmaceutical Chemistry, Comenius University, Odbojarov 10, SK-832 32 Bratislava, Slovakia, and German Cancer Research Center, Im Neuenheimer Feld 280, D-69120 Heidelberg, Germany

Received: July 9, 2007; In Final Form: October 2, 2007

The molecular structure of trimeric units (D−E−F and F−G−H) and the pentamer D−E−F−G−H of heparin (sodium salts and their anionic forms) was studied using the B3LYP/6-31G(d) method. The equilibrium structure of the sodium salts of the trimers and pentamer investigated in the isolated state was determined by multidentate coordination of the sodium cations with oxygen atoms of the sulfate, carboxyl, and hydroxyl (hydroxymethyl) groups, respectively. The displacement of Na^+ ions from the binding sites in the sodium salt of oligosaccharides studied resulted in the appreciable change of the overall conformation of the corresponding anion. Upon dissociation, a large change in both the position of the sulfate groups and the conformation across the glycosidic bonds was observed. The stable energy conformations around the glysosidic bonds found for the pentamer investigated are compared and discussed with the available experimental X-ray structural data for the structurally related heparin-derived pentasaccharides in cocrystals with proteins.

Introduction

Heparin belongs to a family of macromolecules (glycosaminoglycans) found in virtually all tissues in a wide variety of species.[1,2] Sulfo groups in heparin appear to play an important role in various biological effects of this polymer.[3,4] Heparin is used in clinics for the prevention and treatment of thrombosis.[2] Its main antithrombotic activity is explained by its ability to potentiate the activity of serine protease inhibitor antithrombin III (AT-III), which inactivates a number of serine proteases − such as thrombin and factor Xa − in the coagulation cascade.[1,3] However, despite its widespread use for over 60 years as an anticoagulant, heparin's precise 3-D structure, its dynamical behavior, and its certain physical, chemical, and biological properties are still not well-understood. Heparin is composed of repeating 1 → 4 linked uronic acid and glucosamine residues.[5,6] Although the major repeating unit in heparin is a disaccharide, the heparin chain has a high degree of structural variability.[4] Experimental studies suggest that not all of the possible structural variants occur in heparin.[5,6] The action of heparin begins when it binds to antithrombin through a group of five subunits (D−E−F−G−H). It was found that this unique pentasaccharide fragment (PS) constitutes the minimal binding domain for AT-III. It is now possible to synthetically produce the active subunit (D−E−F−G−H) of heparin, which has been recently introduced on the market in the form of its sodium salt.[7]

In spite of their interesting biological properties, the glycosaminoglycans remain one of the structurally less well-characterized classes of saccharides. In the absence of relevant 3-D structural data of heparine salts and their simpler mono- and oligosaccharide derivatives, available experimental structural studies of heparin are limited to these data observed in cocrystals between heparin structural units and proteins. The absence of experimental structural data of basic building units of glycosaminoglycans presents a challenge to the application of molecular modeling methods to obtain insight into the recognition and binding processes. The molecular structures of six monomeric structural units (1-OMe ΔIdoA-2SNa_2 (unit A), 1-OMe GlcN-S6SNa_2 (unit D), 1,4-DiOMe GlcNa (unit E), 1,4-DiOMe GlcN-S3S6SNa_3 (unit F), 1,4-DiOMe IdoA-2SNa_2 (unit G), and 1,4-DiOMe GlcN-S6SNa_2 (unit H)) and four dimeric structural units of heparin (D−E, E−F, F−G, and G−H) have been previously investigated[8−11] using density functional theory.

The present paper reports in detail the structural parameters for two DFT optimized sodium salts of trisaccharides (D−E−F and F−G−H) and the pentasaccharide (D−E−F−G−H) structural units of heparin and their anionic forms using the B3LYP/6-31G(d) method. Of particular interest is the overall shape of sodium salts of oligosaccharides determined by the conformation of the glycosidic linkage and how this shape changes upon sodium cation dissociation and/or in water solution.

Computational Details

The geometry of the sodium salts of the oligosaccharides D−E−F, F−G−H, and D−E−F−G−H, respectively, and their anionic forms (Figure 1), has been completely optimized with the Gaussian 03 program,[12] using the density functional theory[13−15] B3LYP/6-31G(d) method.[16−19] To evaluate the conformational behavior of these molecules in solvents, we carried out optimization calculations in the presence of water. The methodology used in this work is centered on two solvation methods: CPCM[20,21] and Onsager[22] models. Since the initial geometry optimizations of the D−E−F trimer species using the much more computationally expensive conductor polarized continuum model (CPCM) did not converge, in further studies, we decided to utilize the self-consistent reaction field method using the Onsager solvent reaction field (SCRF) model. This model has been implemented and successfully used by Wong et al.[23−26]

* Corresponding author. Tel.: +421-2-50117225; fax: +421-2-50117100; e-mail: remko@fpharm.uniba.sk.
† Comenius University.
‡ German Cancer Research Center.

10.1021/jp075330l CCC: $37.00
Published on Web 12/06/2007

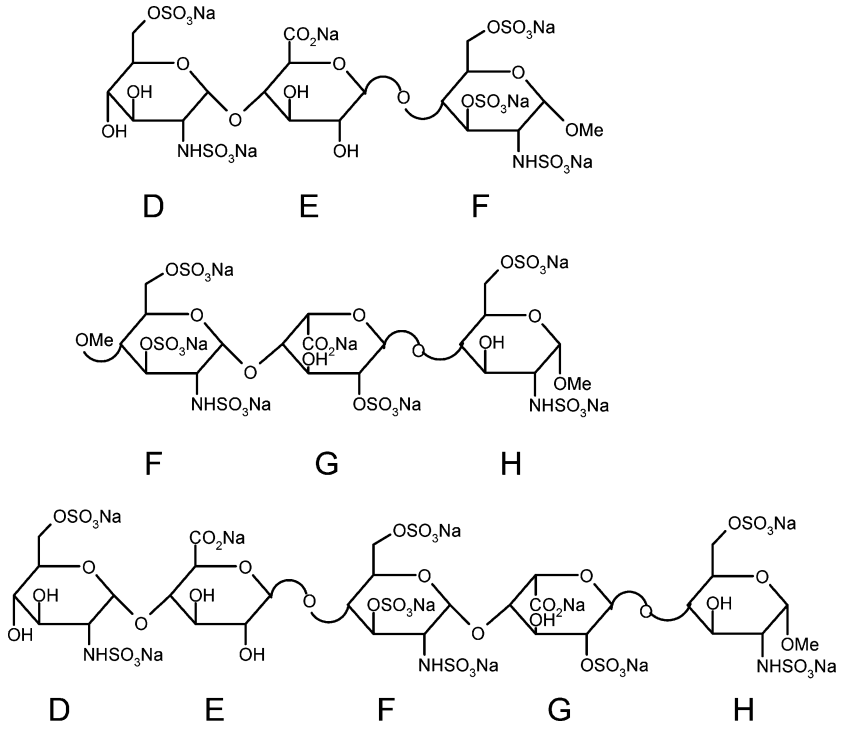

Figure 1. Structure of biologically active pentasaccharide and model trisaccharides investigated.

The interaction energy, ΔE, for the reaction of a sodium cation with Lewis bases [$n\mathrm{Na}^+(g) + \mathrm{L}^{n-}(g) \rightarrow \mathrm{Na}_n\mathrm{L}(g)$] is given by the following equation:

$$\Delta E = E[(\mathrm{Na}^+)_n\cdots\mathrm{L}^{n-}] - \{n\,E[\mathrm{Na}^+] + E[\mathrm{L}^{n-}]\} \quad (1)$$

where $E[\mathrm{Na}^+]$ and $E[\mathrm{L}^{n-}]$ are the energies of the metal cation and ligand molecules, respectively, and $E[(\mathrm{Na}^+)_n\cdots\mathrm{L}^{n-}]$ is the energy of the complex. The structures of all gas-phase and condensed-phase (SCRF) species were fully optimized without any geometrical constraints. It has been shown[27−29] that the density functional theory method yields results, which compare favorably with the corresponding results obtained using a high level, ab initio, coupled-cluster method. Becke's 3LYP method in conjunction with the triple-ζ basis set reproduces thermodynamic quantities[30] of the cation−Lewis base complexes within the targeted accuracy of about 3 kcal mol^{-1}. Hence, DFT is suitable as an alternative to traditional ab initio methods for studying larger metal ion−Lewis base complexes. The values of metal affinities computed using DFT are as good as high level ab initio results and in good agreement with the corresponding experimental data.[30−33]

Results and Discussion

Molecular Structures. The D−E−F and F−G−H trisaccharidic units of the heparin model the pentasaccharide D−E−F−G−H structural unit of a typical fragment of heparin, in which two neighboring structural units of heparin bound by the (1−4) glycosidic bonds are substituted with the methyl groups (Figure 1). The D−E−F−G−H pentamer represents the antithrombin III binding pentasaccharide sequence in heparin. We modeled this sequence by means of the clinically useful synthetic pentasaccharide preparation of fondaparinux sodium.[7] The pyranose rings of D-glucosamine in these oligomers were considered in a more stable $^4C_1$ conformation. The starting conformation of the L-iduronic acid building unit G in oligomers F−G−H and D−E−F−G−H was set to the skew-boat $^2S_0$ form. This conformation was taken as it is the prevalent form of this residue in heparin and its model compounds.[1,3,5,6]

A conformational search using theoretical methods is, for such large systems, limited to the use of some of the available force-field methods. However, there is still no molecular mechanics force-field parametrization capable of adequately reproducing all polysaccharide conformational features.[3,34] It is common in the computational study of carbohydrates to use structural data obtained from X-ray crystallography or NMR spectroscopy as guides to the quality of the theoretical computations. Initial conformations using the DFT calculations of the oligomers studied were constructed by means of the Gauss View graphical interface of Gaussian. The relative orientation of pyranose rings defined by two torsion angles (Φ and Ψ) at the 1 → 4 glycosidic linkage was taken from the experimental data for structurally related oligosaccharides containing D−E−F−G−H fragments of heparin.[35,36] The appropriate number of sodium counterions was added to each unit at positions derived from previous studies of similar model systems.[8−11,37−39]

The Cartesian coordinates (Å) of all gas-phase oligomers investigated, optimized at the B3LYP/6-31G(d) level of theory, are given in Table A of the Supporting Information. To check the correctness of the B3LYP calculated structures using the double-ζ basis set, especially the geometry of the sodium bridges, we also performed full geometry optimization of the trimer D−E−F (Table A of the Supporting Information), using the basis set of the triple-ζ quality (B3LYP/6-31++G(d,p) level of theory). Examination of the space models of the B3LYP computed structures using two basis sets of this trimer shows that the increase of the basis set gives essentially the same results. However, the overall shape of the molecular structure of the neutral sodium salts of the D−E−F, F−G−H, and D−E−F−G−H oligomers is stabilized via multidentated Na···O sodium bonds. The ionization of the respective sodium salts results in structural rearrangements of polyanions.

With the aim to study the influence of the surrounding medium on the stability of the glycosaminoglycans studied, we

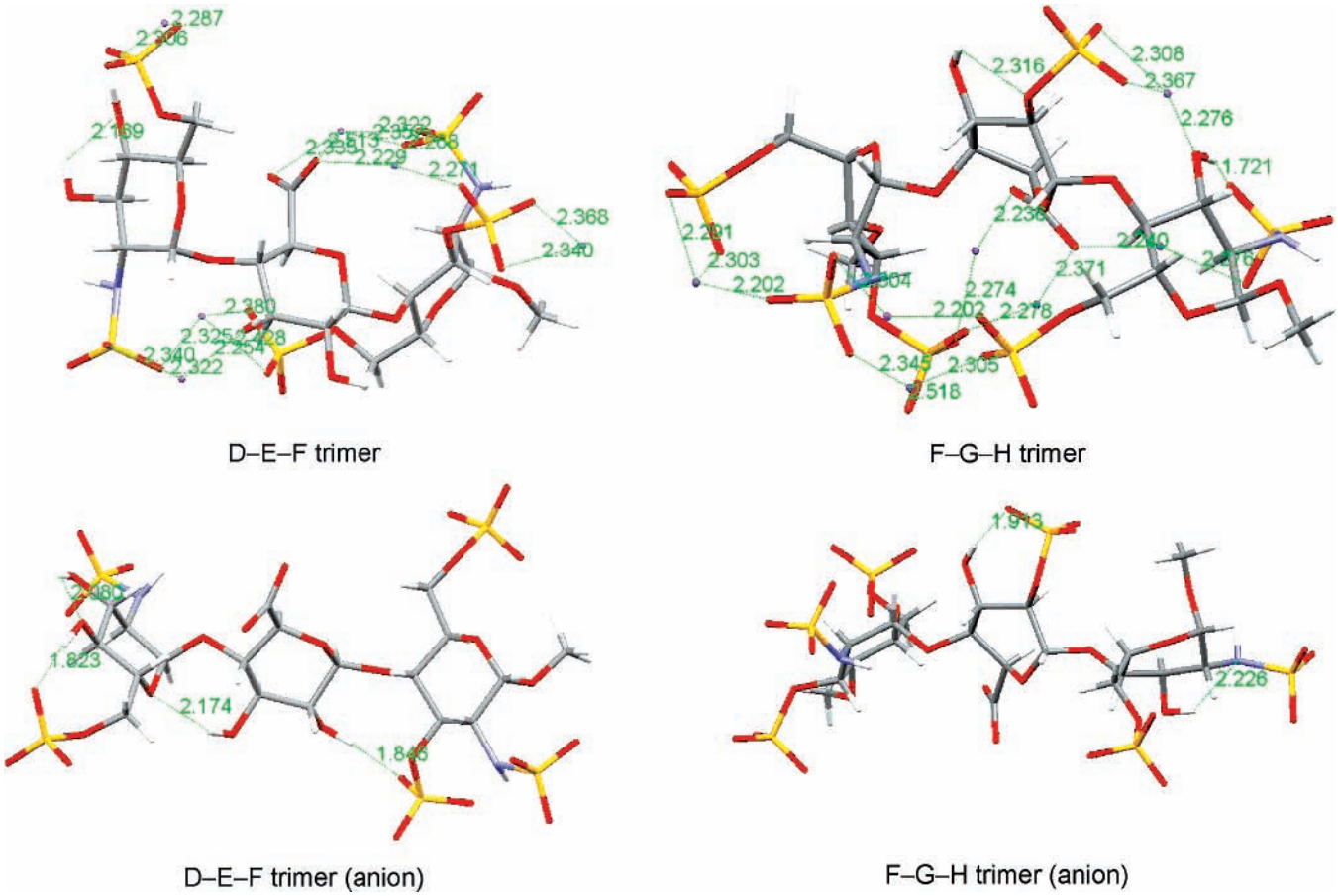

Figure 2. Lowest energy structures of the D−E−F and F−G−H trisaccharide species in water solution. Sodium cations are purple.

also investigated the environmental effects. The calculations were carried out, for computational reasons, using the SCRF formalism of Wong et al.[23−26] The radii of the cavities used in this approach were chosen after a volume calculation of each molecule, and the dielectric constant of water ($\epsilon = 78.5$) was used. The placing of the isolated molecules into a spherical cavity within a dielectric medium of the Onsager model of solvation does not represent the realistic situation in the biological medium; it seems helpful in revealing the main role of the solvent in intermolecular electrostatic interactions. Water has a remarkable effect on the geometry of glycosaminoglycans, especially their anions.

Trimer D−E−F. In the trimer D−E−F, the overall shape of the molecular structure was stabilized via the sodium bonds originating between oxygen atoms of the $C(2)NHSO_3^-$ group of unit D and the $C(4)C(5)OSO_3^-$ moiety in unit F. In addition to this, the two sodium cations of the $C(5)CO_2^-$ group (unit E) and the $C(2)NHSO_3^-$ group of unit F form a second multicoordinated network of coordination bonds interconnecting the electronegative oxygen atoms of these groups. The C(3)OH group of unit D is involved in the intramolecular hydrogen bond of the C(3)OH···O−C(3) network. The gas-phase structure of the hexaanion of this trimer is stabilized by three intramolecular hydrogen bonds formed by the hydroxyl groups of subunits D and E. These hydrogen bonds are preserved also in solution (Figure 2).

Trimer E−F−G. The gas-phase structure of the neutral molecule is also presented in the Supporting Information. Seven Na^+ cations of this trimer are multicoordinated with sulfate and carboxyl groups of individual pyranose rings. Optimal Na^+···O distances are in a relatively short range of 2.2−2.4 Å and result in unique stabilization of the glycosidic bonds. The overall structure is stabilized by means of two intramolecular hydrogen bonds: C(3)OH···OSO_3^- and C(3)OH···$^-OSO_2NHC(2)$. This bonding pattern is also preserved in the solvated structure. A different conformation is found with the gas-phase anion. Dissociation of the seven Na^+ cations results in the conformational change of the side sulfate groups. In the absence of the interring stabilization via hydrogen bonds, the overall anion geometry is a result of the net repulsion among the anionic substituent groups (Figure 2).

Pentamer D−E−F−G−H. The geometry of the optimized sodium salt of the pentamer D−E−F−G−H is also presented in the Supporting Information. As long as the Na^+ cations in the simpler models of the glycosaminoglycan functional groups (CH_3CO_2Na, CH_3OSO_3Na, and CH_3NHSO_3Na) always form bifurcated coordination bonds with two oxygen atoms of the Lewis base[11] for the pentamer studied, the formation of the multiple coordination bonds of 10 Na^+ cations with the pentasaccharide substituent groups is characteristic. However, it is known that the metal ion affinity of glycosaminoglycans is greatly affected by the geometrical features of the site of recognition, stereo effects, and type of noncovalent interactions that can be formed at or near the binding group.[3] There are two physically distinct models of ion binding to polynucleotides and glycosaminoglycans: site-specific and nonspecific electrostatic binding.[40−43] Site-specific binding involves a specific close carboxylate, *N*- and *O*-sulfate anion−cation complexes. The inspection of the network of the sodium coordination bonds in the pentasaccharide sodium using the Gauss View software shows that the Na^+ atoms in general do not form site-specific coordination bonds. The favored pentasaccharide Na_{10} structure contains D, E, F, G, and H pyranose rings in such mutual positions that permit tri- or tetradentate Na^+ coordination. One

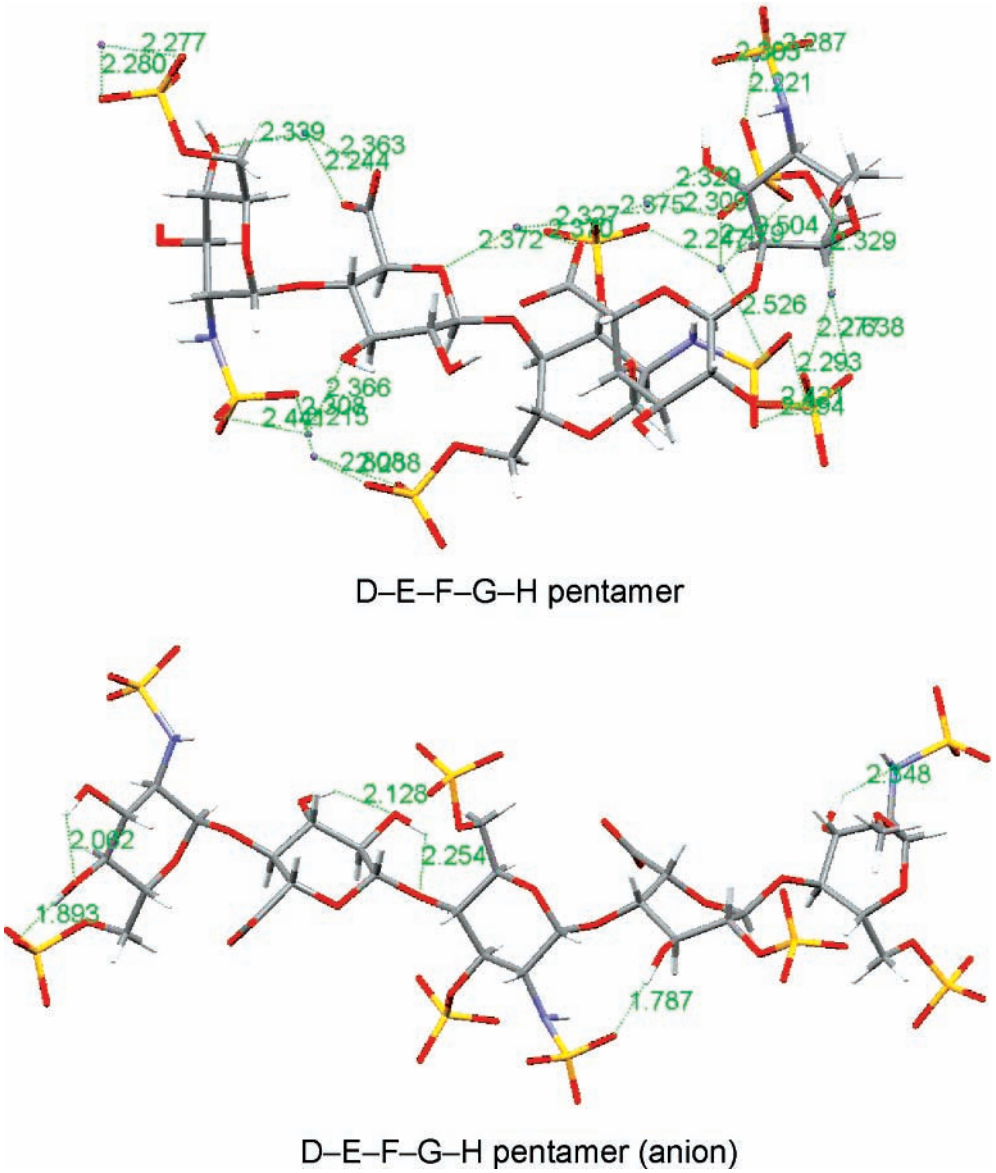

Figure 3. Lowest energy structures of the D−E−F−G−H pentasaccharide species in water solution. Sodium cations are purple.

exception is the C(5)OSO_3Na moiety of the pyranose D ring, in which the Na^+ atom forms with the sulfate group the bifurcated coordination bond only. The network of these coordination bonds is also preserved in the solvated salt of pentasaccharide (Figure 3). The overall structure of the pentasaccharide sodium is rather bent, and the hydroxyl groups of the units D, E, F, and H are involved in the intramolecular hydrogen bonds of the O−H···O network. The investigation[44] of the structure of Na^+ coordinated mono- and disaccharides reveals that even the simple saccharides coordinate a Na^+ cation in a multidentate mode (≥ 2).

For the manifestation of the changes in the molecular structure of the sodium pentameric glycosaminoglycans upon dissociation and/or solvent effects, we used the molecular structure of the sodium pentasaccharide D−E−F−G−H. The superposition of the selected 3-D structures of this saccharide is presented in Figure 4. The presence of the 10 negatively charged groups in this system increases their interaction with the counterions (Na^+) of the surrounding medium. The minimum energy molecular structure of sodium pentasaccharide, due to the interaction of the Na^+ ions with its ionic sites, represents a rather bent structure. The ^{23}Na relaxation data indicate that Na^+ ions are displaced by cationic centers upon binding of the corresponding

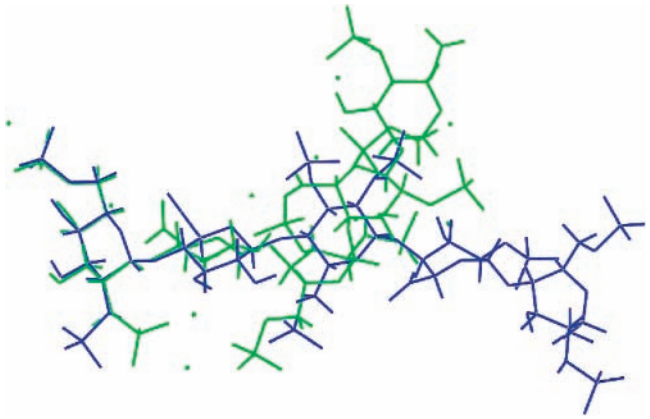

Figure 4. Molecular superimposition of the in solution optimized sodium salt of the pentamer D−E−F−G−H (green) and its anion (blue).

segment of heparine to model peptides. This binding involves both delocalized and direct electrostatic interactions between cationic groups of proteins and anionic sites of heparin.[45] The displacement of the Na^+ ions from the binding sites in the sodium salt of the pentasaccharide studied results in the

TABLE 1: B3LYP/6-31G(d) Optimized Glycosidic Bond Angles (deg) of Trimers and Pentamer Studied

	D−E−F					F−G−H				D−E−F−G−H (fondaparinux)			
angle	Na salt[a]	Na salt	solvated Na salt	anion	solvated anion	Na salt	solvated Na salt	anion	solvated anion	Na salt	solvated Na salt	anion	solvated anion
Φ_1	59.5	58.8	53.4	55.7	55.4					63.7	63.9	66.1	67.0
ψ_1	−140.5	−138.2	−146.8	−176.0	−179.3					−169.8	−171.5	−158.3	−157.1
Φ_2	−54.7	−55.0	−57.0	21.6	19.6					−124.8	−127.3	−86.8	−88.7
ψ_2	−114.1	−113.6	−110.1	−118.0	−116.6					−77.7	−75.8	−92.3	−91.7
Φ_3						51.1	49.6	63.3	62.7	54.3	53.3	77.2	77.0
ψ_3						−157.5	−157.4	−156.0	−153.5	−175.9	−173.6	−152.4	−152.4
Φ_4						−35.8	−33.6	−85.2	−94.8	−69.1	−70.9	−90.9	−90.4
ψ_4						−95.6	−96.4	−80.5	−72.2	−127.1	−127.4	−90.9	−89.8
Φ_{H1}	−56.1	−56.7	−61.6	−60.2	−60.4					−54.4	−54.2	−50.6	−49.7
ψ_{H1}	−23.3	−21.0	−28.4	−63.6	−66.8					−52.9	−54.5	−41.4	−40.0
Φ_{H2}	65.2	64.6	61.7	140.4	138.5					−5.3	−8.0	37.8	35.9
ψ_{H2}	2.4	2.7	6.6	2.3	3.8					42.2	43.8	31.1	31.5
Φ_{H3}						−67.6	−68.9	−52.7	−53.8	−65.2	−66.1	−37.1	−37.7
ψ_{H3}						−37.6	−37.6	−39.0	−35.8	−57.7	−55.5	−34.1	−34.2
Φ_{H4}						80.9	83.2	32.9	23.5	49.4	47.9	26.4	26.8
ψ_{H4}						26.8	25.7	39.2	48.8	−11.2	−11.5	28.4	29.5

[a] B3LYP/6-31++G(d,p) calculation.

appreciable change of the overall conformation of the corresponding anion. Upon dissociation, a large change in both the position of the sulfate groups and the conformation across the glycosidic bonds is observed. The hydroxyl groups of the pentamer anion are involved in H-bonding (Figure 3). The conformation across the glycosidic bond connecting pyranose rings F and G is stabilized by the C(3)OH···OSO_2NHC(2) hydrogen bond. Other hydroxyl groups of individual saccharide units are involved in H-bonding within the pyranose ring. This hydrogen bond pattern is also preserved in the solvated pentasaccharide anion (Figure 5).

Structure of Glycosidic Linkage. For the definition of the torsion angles at the glycosidic bonds, we used the recommendations and symbols of nomenclature proposed by IUPAC.[46] The relative orientation of a pair of dimers studied is described by two torsional angles at the glycosidic linkage, denoted Φ and Ψ. For a 1 → 4 linkage, the definitions of these torsion angles are as follows: Φ = O(5)−C(1)−O(1)−C(4′) or Φ_H = H(1)−C(1)−O(1)−C(4′) and Ψ = C(1)−O(1)−C(4′)−C(5) or Ψ_H = C(1)−O(1)−C(4′)−H(4′). The glycosidic bond angles of the fully optimized trimers D−E−F and F−G−H and pentamer D−E−F−G−H are given in Table 1. The equilibrium structure of the sodium salts of the trimers and pentamer investigated in the isolated state was determined by the multidentate coordination of the sodium cations with oxygen atoms of the sulfate, carboxyl, and hydroxyl (hydroxymethyl) groups, respectively. This specific interaction gives rise to the unique overall shape of individual oligomers (Figures 2 and 3) and is manifested by the computed values of the Φ and Ψ torsion angles of the glycosidic linkage. Values of these glycosidic angles for individual trimers are considerably different (Table 1). From the molecular structure of the trimers studied (Figure 2), it is clear that the sodium cations are involved in screening of negative charges of trisaccharide structural units of heparin. Different attractive forces between Na^+ cations and functional sulfate, carboxyl, and hydroxyl groups of the trimers D−E−F and F−G−H stabilize the equilibrium conformation at the glycosidic bonds. In neutral sodium salts, ionic interactions are dominant as the negatively charged sulfate and carboxyl groups form multidentate coordination bonds with Na^+ cations. In the absence of the solvating effect of the Na^+ cations, the anions of the trimers D−E−F and F−G−H adopt a different conformation. The overall structure of the gas-phase anions is a compromise between the repulsion forces of anions and the H-bonding pattern in both trimers. Previous calculations of D−E, E−F, F−G, and G−H dimers, respectively, with the B3LYP DFT method[9] reached considerably different individual glycosidic torsion angles. Thus, the 3-D structure of the higher oligomers of heparin cannot be deduced from the known conformation of the basic dimeric units. The same is true for the D−E−F and F−G−H trimeric units of heparin. There are large differences in computed equilibrium torsion angles for trimeric and pentameric D−E−F−G−H structure, respectively. Only the torsion angles Φ_1 and Φ_3 are close to each other in three oligosaccharides investigated (Table 1).

As regards of the fondaparinux sodium (pentamer D−E−F−G−H), the dissociation of the saccharide−sodium bonds is connected with the large change of the overall 3-D structure. For both gas-phase and hydrated polyanion, the extended structure of the uniform helical conformation is the most stable one. The calculated helical parameter *h* (the axial rise per pentasaccharide) was as follows: 18.51 Å with solvated fondaparinux sodium and 22.02 Å in solvated polyanion of the fondaparinux. Inter-ring orientations in these oligomers are significantly influenced by the coordination of sodium cations, ionization, and/or solvent effect. The computed structural data can be directly compared with the gas-phase data for isolated systems and/or experimental data for molecules measured in a water solution. However, to our knowledge, no experimental 3-D structural parameters have been available until now. In the absence of experimental (gas-phase) data for the oligomers studied, the geometry of parent molecules can be compared only with X-ray data on structurally related pentasaccharides in their complexes with proteins (Table 2), namely, natural pentasaccharide D−E−F−G−H (in the complex of antithrombin with pentasaccharide D−E−F−G−H[47] and X-ray experimental data for antithrombin in the pentasaccharide-bound intermediate state[48]) and the synthetic version of the naturally occurring pentasaccharide fondaparinux (in the complex with antithrombin and coagulation factor Xa[49]). The values of the glycosidic angles of these pentasaccharides are also listed in Table 2.

In the solid state, the pentasaccharide is bound to the protein in the form of an anion. The solid-state structure of pentasaccharide can be affected by so-called packing effects, which can distort the structure. The solved cocrystal structures of pentasaccharide with proteins have highlighted the ionic interactions between specific sulfate groups and carboxyl groups of pentasaccharide with the basic amino acids of binding site on the

TABLE 2: B3LYP/6-31G(d) Optimized Glycosidic Bond Angles (deg) of Fondaparinux Sodium, Its Anion, and Experimental Structural Data of Related Pentasaccharides in Their Complexes with Proteins

	D−E−F−G−H (fondaparinux), calcd				D−E−F−G−H, exptl[a]			
angle	Na salt	solvated Na salt	anion	solvated anion	1AZX[b]	1E03[b]	1NQ9[c]	2GD4[d]
Φ_1	63.7	63.9	66.1	67.0	89.3 (91.0)	84.7 (96.9)	81.5 (77.7)	101.4
ψ_1	−169.8	−171.5	−158.3	−157.1	−141.4 (−154.1)	−137.0 (−153.7)	−137.6 (−142.6)	−157.6
Φ_2	−124.8	−127.3	−86.8	−88.7	−86.0 (−79.6)	−87.3 (−72.4)	−89.0 (−86.5)	−84.4
ψ_2	−77.7	−75.8	−92.3	−91.7	−112.7 (−118.8)	−112.5 (−116.8)	−108.6 (−107.4)	−120.8
Φ_3	54.3	53.3	77.2	77.0	55.4 (49.1)	58.7 (45.7)	59.2 (58.4)	63.1
ψ_3	−175.9	−173.6	−152.4	−152.4	−154.4 (−153.2)	−164.1 (−151.1)	−162.1 (−159.5)	−157.0
Φ_4	−69.1	−70.9	−90.9	−90.4	−69.8 (−74.0)	−63.4 (−78.1)	−62.1 (−69.8)	−67.8
ψ_4	−127.1	−127.4	−90.9	−89.8	−115.2 (−103.8)	−119.6 (−92.8)	−121.4 (−119.8)	−108.5

[a] X-ray structure of the second molecule in the asymmetric unit is in parentheses. [b] Values of experimentally determined Φ and Ψ torsional angles for the complex of antithrombin with pentasaccharide.[47] [c] X-ray experimental data for antithrombin in the pentasaccharide-bound intermediate state.[48] [d] Pentamer (fondaparinux) anion from cocrystal with antithrombin and coagulation factor Xa.[49]

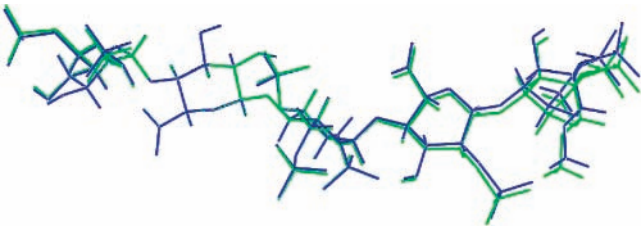

Figure 5. Molecular superimposition of the gas-phase pentamer D−E−F−G−H anion (green) and in solution optimized anion of the pentamer D−E−F−G−H (blue).

protein.[47−50] However, ionic contacts are not sufficient to explain the optimal structural fit of pentasaccharide to the binding site of protein that influences the affinity of the interaction. It is assumed that binding of the pentasaccharide to the protein would also induce local distorsions in an otherwise uniform helical structure of pentasaccharide, which are manifested as changes in the glycosidic torsion angles. The naturally related pentasaccharide conformations in cocrystals with different proteins and/or environments (PDB files 1AZX, 1E03, and 1NQ9) represented by the glycosidic torsion angles are close to each other (Table 2). However, the experimentally determined torsion angles at the glycosidic linkage of the pentasaccharide fondaparinux in its complex with antithrombin and the coagulation factor Xa (PDB file 2GD4) are slightly different (Table 2), indicating that the fine differences in the ionic interactions resulting from the different patterns of the sulfate, carboxyl, and methoxy substituents of these two pentasaccharides also contribute to the optimal structural fit of these compounds to the binding site of the protein.

The experimentally determined 3-D structure of the pentasaccharide studied corresponds to the bound molecule at the protein; therefore, the general structural motifs of the pentasaccharide can be compared with results for isolated molecules from theoretical methods only. The experimental values for the glycosidic angles in the pentasacharide−protein complexes are well-interpreted by the corresponding angles computed for solvated anions of the fondaparinux sodium. Despite the fact that some of the torsion angles computed by us for the anion of fondaparinux sodium (e.g., angles Ψ_1, Φ_2, and Ψ_3) proved to be close to the experimentally determined torsion angles in the cocrystal of this anion (Table 2), the overall structure of the bound and unbound pentasaccharide is very different (Figures 6 and 7). The experimental helical parameter *h* (the axial rise per pentasaccharide) is in the cocrystal of the pentasaccharide fondaparinux with antithrombin and coagulation factor Xa equal to 21.51 Å, which is close to the analogous value computed for the solvated anion of the fondaparinux

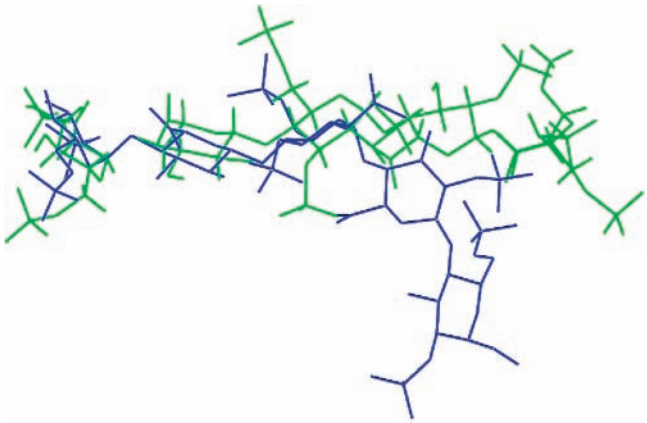

Figure 6. Molecular superimposition of the in solution optimized anion of the pentamer D−E−F−G−H (green) and pentamer anion from the cocrystal with antithrombin and coagulation factor Xa, PDB2GD4 (blue).

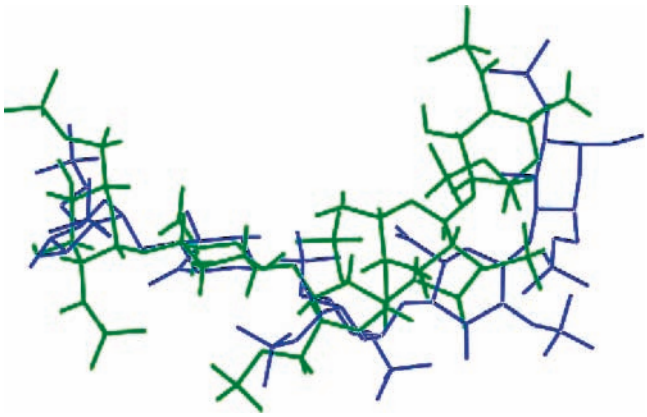

Figure 7. Molecular superimposition of the pentasaccharide sodium salt D−E−F−G−H (green) and pentamer anion from the cocrystal with antithrombin and coagulation factor Xa, PDB2GD4 (blue).

(22.02 Å). Thus, the equilibrium conformation of the pentasaccharide bound to the protein occurs between two extreme positions, namely, the thermodynamically stable conformation of the neutral pentasaccharide−sodium$_{10}$ salt and its anion. The computed torsion glycosidic angles (Φ_1 and Ψ_2) and (Φ_2 and Ψ_2) for the rotation of the D−E and E−F units in the pentasaccharide studied (Table 2) fit well the available experimentally (NMR spectroscopy) determined glycosidic angles (−49 and −31) and (43 and 12), respectively, in structurally related hexasaccharide.[51]

Gas-Phase Sodium Affinities. The calculated gas-phase Na^+ affinities (interaction energies) of the sodium salts of the trimers

TABLE 3: B3LYP/6-31G(d) Calculated Gas State and Solvated-Phase Na^+ Affinities in Oligommers Studied (kcal mol^{-1})

	total Na^+ affinity		affinity per Na^+		
species	gas phase	in water	gas phase	in water	no. of Na^+ bonds
D−E−F	−1432.6	−1456.8	−238.8	−242.8	6
F−G−H	−1861.7	−1858.8	−266.0	−265.5	7
D−E−F−G−H (fondaparinux sodium)	−2955.4	−2966.3	−295.5	−296.6	10

D−E−F, F−G−H, and pentamer D−E−F−G−H are given in Table 3. No corrections for basis set superposition errors (BSSE) were incorporated into the results since B3LYP calculations of the Na^+ affinities for structurally related dimmers D−E, E−F, F−G, and G−H, respectively, with the larger basis set 6-311++G(d, p) changed the interaction energy only slightly.[9] Thus, the basis set used here is adequate to reduce the basis set superposition error effects. The computed sodium affinities represent values for the dissociation of several sodium monocations from their binding sites (carboxyl and sulfate groups). For reasons of comparison of the contribution of the individual Na^+ cations to the interaction energies, the sodium affinity per Na^+ cation is also presented. The largest interaction energy per Na^+ cation was found in pentamer D−E−F−G−H. Inter-ring orientation in this pentamer is considerably stabilized by the system of coordination bonds formed by 10 Na^+ ions and functional groups of the hexose rings. Sodium cations are also involved in the stabilization of the inter-ring conformation of trimers D−E−F and F−G−H. The ionization of the sodium salts of the trimers and pentamer studied is associated with considerable conformational rearrangements of ionic species (Figures 2−4). This rearrangement is responsible for an additional energetic stabilization of anionic species. Heparin has been recognized to bind to the receptor proteins mostly through its anionic (carboxylate, *N*−- and *O*-sulfate) groups of the unique pentasaccharide moiety.[3] The ab initio calculations of the monomeric unit of heparin[8] (1,4-DiOMe IdoA2S sodium salt) have shown that the breaking of the sodium bonds in the glycosaminoglycans is costly in terms of enthalpy but results in an appreciable gain in entropy. It is assumed that much of the Gibbs energy of interaction of heparin and its derivatives with proteins should be derived (like DNA) from the entropically favorable release of Na^+ ions.[3] It is well-known that the adhesion of alkaline and alkaline-earth cations to basic centers results in the formation of essentially electrostatic bonds.[3] In addition to electrostatic interactions, the dielectric properties of the environment play an important role in the process of metal cation binding. The Gibbs energies and enthalpies for lithium and sodium cations binding to the anionic molecule (structural unit G of heparin modeled by the 1,4-DiOMe IdoA-2S^{2-}, ^2S_o conformation) studied in aqueous solution were recently computed by us.[11] In the gas phase, the binding reactions could occur with high Gibbs binding energies. This is due to the strong attractive Coulombic interactions between the oppositely charged Li^+ and Na^+ cations and the carboxylate and sulfate groups, respectively. The binding enthalpy in the gas phase is substantially larger in magnitude than in a polar solvent (water). The computed binding enthalpies in water solution (CPCM model of solvent) are low and negative (i.e., stabilizing). However, the entropy term is always high and negative, opposing association. The computed Gibbs binding energies for the 1,4-DiOMe IdoA-2SM (M = Li^+, Na^+) in aqueous solutions range from 31 to 50 kJ mol^{-1}. Thus, there is little tendency for the salts to associate by means of Li^+···ligand and Na^+···ligand ionic bonds, and in a water-exposed environment, the high hydration effect between sodium (lithium) cations and anions results in a diminution of the direct electrostatic and ion−dipole interactions. The computed sodium affinities of the trimers and pentamer studied in water using the SCRF theory by the Osanger dipole method are almost the same as those values for the gas phase (Table 3). However, it is well-known that the simple Onsager dipole method is not able to correctly describe all of the electronic aspects of the strong solute, that is, −solvent interactions (e.g., hydrogen bonding between solvent (water) and solute (saccharide)).

In our previous investigations[8−11] the role of solvent on the geometry and molecular equilibria of the monomer and dimeric structural units of heparin was analyzed by using the self-consistent reaction field methods (CPCM or Poisson−Boltzmann solver of Jaguar). However, for more exact calculations of the effect of solvent (water) on the structure and energy of the salts of glycosaminoglycans it is necessary to treat at least the first solvation shell explicitly. Calculations of monomeric and oligomeric units of heparin using the supermolecule, and the hybrid supermolecule-continuum models, are also in progress in our laboratory.

Conclusion

This theoretical study set out to determine stable conformations of D−E−F and F−G−H trimers, D−E−F−G−H pentamer, and their ionized forms. For these oligomers of heparin, experimental physicochemical data that consider their chemical and biological importance are scare. The following conclusions can be drawn.

(1) The overall shape of the molecular structure of the neutral sodium salts of the D−E−F, F−G−H, and D−E−F−G−H oligomers is stabilized via multidentated Na···O sodium bonds. The ionization of the respective sodium salts results in structural rearrangements of polyanions.

(2) The displacement of the Na^+ ions from the binding sites in the sodium salt of the pentasaccharide studied results in the appreciable change of the overall conformation of the corresponding anion. Upon dissociation, a large change in both the position of the sulfate groups and the conformation across the glycosidic bonds was observed.

(3) Previous calculations[9] of D−E, E−F, F−G, and G−H dimers, respectively, with the B3LYP DFT method, reached considerably different individual glycosidic torsion angles. Thus, the 3-D structure of the higher oligomers of heparin cannot be deduced from the known conformation of the basic dimeric units. The same is true for the D−E−F and F−G−H trimeric units of heparin. There are large differences in computed equilibrium torsion angles for trimeric and pentameric DEFGH structures, respectively.

(4) In neutral sodium salts, ionic interactions are dominant as the negatively charged sulfate and carboxyl groups form multidentate coordination bonds with Na^+ cations. The largest interaction energy per Na^+ cation was found in the pentamer D−E−F−G−H. Inter-ring orientation in this pentamer was considerably stabilized by the system of coordination bonds formed by 10 Na^+ ions and functional groups of hexose rings.

(5) This work yields quantities that may be inaccessible or complementary to experiments and represents the first quantum chemical approach in which both the gas-phase and the solvated-phase 3-D structure of the trimeric and pentameric units of heparin were determined.

(6) Complexation between sodium cation and carboxylate, *N*- and *O*-sulfate anions, of the basic structural units of heparin were considered, and absolute metal ion affinities were evaluated.

Acknowledgment. This research was supported by the Slovak Ministry of Education (to M.R., VEGA Grant 1/4301/07). The calculations were performed using the DKFZ HPC resources during M.R.'s stay in Heidelberg as a DKFZ guest scientist.

Supporting Information Available: B3LYP/6-31G(d) optimized Cartesian coordinates (Å) of all gas-phase trimers and pentamer investigated. This material is available free of charge via the Internet at http://pubs.acs.org.

References and Notes

(1) Rodén, L. In *Heparin-Chemical and Biological Properties*; Lane, D. A., Lindahl, U., Eds.; CRC Press: Boca Raton, FL, 1989; pp 1−24.
(2) Desai, U. R. *Med. Res. Rev.* **2004**, *24*, 151.
(3) Capila, I.; Linhardt, R. J. *Angew. Chem., Int. Ed.* **2002**, *41*, 390.
(4) Rabenstein, D. L. *Nat. Prod. Rep.* **2002**, *19*, 312.
(5) Lane, D. A.; Lindahl, U. *Heparin-Chemical and Biological Properties*; CRC Press: Boca Raton, FL, 1989.
(6) Casu, B.; Lindahl, U. *Adv. Carbohydr. Chem. Biochem.* **2001**, *57*, 159.
(7) Petitou, M.; van Boeckel, C. A. A. *Angew. Chem., Int. Ed.* **2004**, *43*, 3118.
(8) Remko, M.; von der Lieth, W. C. *J. Chem. Inf. Mod.* **2006**, *46*, 1194.
(9) Remko, M.; von der Lieth, W. C. *J. Chem. Inf. Mod.* **2006**, *46*, 1687.
(10) Remko, M.; Swart, M.; Bickelhaupt, F. M. *J. Phys. Chem. B* **2007**, *111*, 2313.
(11) Remko, M.; van Duijnen, P. T.; von der Lieth, W. C. *J. Mol. Struct. (THEOCHEM)* **2007**, *814*, 119.
(12) Frisch, M. J. et al. *Gaussian 03*, Revision B.04; Gaussian, Inc.: Pittsburgh, PA, 2003.
(13) Kohn, W.; Sham, L. J. *Phys. Rev. A: At., Mol., Opt. Phys.* **1965**, *140*, 1133.
(14) For a recent perspective, see: Baerends, E. J. *Theor. Chem. Acc.* **2000**, *103*, 265.
(15) Bickelhaupt, F. M.; Baerends, E. J. In *Reviews in Computational Chemistry*; Lipkowitz, K. B., Boyd, D. B., Eds.; Wiley-VCH: New York, 2000; Vol. 15, pp 1−86.
(16) Becke, A. D. *Phys. Rev. A: At., Mol., Opt. Phys.* **1988**, *38*, 3098.
(17) Becke, A. D. *J. Chem. Phys.* **1993**, *98*, 5648.
(18) Lee, C.; Yang, W.; Parr, R. G. *Phys. Rev. B: Condens. Matter Mater. Phys.* **1988**, *37*, 785.
(19) Hehre, W. J.; Radom, L.; Schleyer, P. v. R.; Pople, J. A. *Ab Initio Molecular Orbital Theory*; Wiley: New York, 1986.
(20) Barone, V.; Cossi, M. *J. Phys. Chem. A* **1998**, *102*, 1995.
(21) Cossi, M.; Rega Scalmani, G.; Barone, V. *J. Comput. Chem.* **2003**, *24*, 669.
(22) Onsager, L. *J. Am. Chem. Soc.* **1936**, *58*, 1486.
(23) Wong, M. W.; Frisch, M. J.; Wiberg, K. B. *J. Am. Chem. Soc.* **1991**, *113*, 4776.
(24) Wong, M. W.; Frisch, M. J.; Wiberg, K. B. *J. Am. Chem. Soc.* **1992**, *114*, 523.
(25) Wong, M. W.; Frisch, M. J.; Wiberg, K. B. *J. Chem. Phys.* **1991**, *95*, 8991.
(26) Wong, M. W.; Frisch, M. J.; Wiberg, K. B. *J. Am. Chem. Soc.* **1992**, *114*, 1645.
(27) Johnson, B. G.; Gill, P. M. W.; Pople, J. A. *J. Chem. Phys.* **1993**, *98*, 5612.
(28) Oliphant, N.; Bartlett, R. J. *J. Chem. Phys.* **1994**, *100*, 6550.
(29) Kapp, J.; Remko, M.; Schleyer, P. v. R. *J. Am. Chem. Soc.* **1996**, *118*, 5745.
(30) Alcamí, M.; González, A. I.; Mó, O.; Yánez, M. *Chem. Phys. Lett.* **1999**, *307*, 244.
(31) Remko, M. *Mol. Phys.* **1997**, *91*, 929.
(32) Remko, M.; Rode, B. M. *J. Mol. Struct. (THEOCHEM)* **2000**, *505*, 269.
(33) Remko, M.; Rode, B. M. *J. Phys. Chem. A* **2006**, *110*, 1960.
(34) Dyekjær, J. D.; Rasmussen, K. *Mini-Rev. Med. Chem.* **2003**, *3*, 713.
(35) DiGabriele, A. M.; Lax, I.; Chen, D. I.; Svahn, C. M.; Jayes, M.; Schlessinger, J.; Hendrickson, W. A. *Nature (London, U.K.)* **1998**, *393*, 812.
(36) Mulloy, B.; Linhardt, R. J. *Curr. Opin. Struct. Biol.* **2001**, *11*, 623.
(37) Lamba, D.; Glover, S.; Mackie, W.; Rashid, A.; Sheldrick, B.; Pérez, S. *Glycobiology* **1994**, *4*, 151.
(38) Ojala, W. H.; Albers, K. E.; Gleason, W. B.; Choo, C. G. *Carbohydr. Res.* **1995**, *275*, 49.
(39) Yates, E. A.; Mackie, W.; Lamba, D. *Int. J. Biol. Macromol.* **1995**, *17*, 219.
(40) Felsenfeld, G.; Miles, T. H. *Annu. Rev. Biochem.* **1967**, *36*, 407.
(41) Whitfield, D. M.; Stojkovski, S.; Sarkar, B. *Coord. Chem. Rev.* **1993**, *122*, 171.
(42) Rabenstein, D. L.; Robert, J. M.; Peng, J. *Carbohydr. Res.* **1995**, *278*, 239.
(43) Chevalier, F.; Lucas, R.; Angulo, J.; Lomas, M. M.; Nieto, P. M.; *Carbohydr. Res.* **2004**, *339*, 975.
(44) Cerda, B. A.; Wesdemiotis, C. *Int. J. Mass Spectrom.* **1999**, *189*, 189.
(45) Hari, S. P.; McAllister, H.; Chuang, W.-L.; Christ, M. D.; Rabenstein, D. L. *Biochemistry* **2000**, *39*, 3763.
(46) http://www.chem.qmul.ac.uk/iupac/2carb/.
(47) Jin, L.; Abrahams, J. P.; Skinner, R.; Petitou, M.; Pike, R. N.; Carrell, R. W. *Proc. Natl. Acad. Sci. U.S.A.* **1997**, *94*, 14683.
(48) Johnson, D. J. D.; Huntington, J. A. *Biochemistry* **2003**, *42*, 8712.
(49) Johnson, D. J. D.; Li, W.; Adams, T. E.; Huntington, J. A. *EMBO J.* **2006**, *25*, 2029.
(50) Raman, R.; Sasisekharan, V.; Sasisekharan, R. *Chem. Biol.* **2004**, *12*, 267.
(51) Mikhailov, D.; Linhardt, R. J.; Mayo, K. H. *Biochem. J.* **1997**, *328*, 51.